For student paper competition

Cognitive Radar for Target Tracking in Multipath Scenarios

Phani Chavali, *Student Member, IEEE* and Arye Nehorai*, *Fellow, IEEE*
Department of Electrical and Systems Engineering
Washington University in St. Louis
One Brookings Drive, St. Louis, MO 63130, USA
Email: {chavalis, nehorai}@ese.wustl.edu
Phone: 314-935-7520 Fax: 314-935-7500

Abstract— **In this paper, we propose a cognitive radar system for target tracking in the presence of multipath reflections. We exploit the inherent spatial diversity offered by the multipath environment by constructing a new measurement vector, which we refer to as a virtual measurement vector. We employ broadband Orthogonal Frequency Division Multiplexing (OFDM) signalling at the transmitter and implement adaptive waveform design by minimizing the posterior Cramér Rao bound (PCRB) on the target state estimates to find the optimal weights to be transmitted on each subcarrier bin of the OFDM signal. We demonstrate with numerical simulations that the mean square error in the case of a cognitive radar is significantly lower than the mean square error in the case of a standard radar.**

I. Introduction

Cognitive radar is a relatively new concept to the radar community [1]. Advances in the field of reconfigurable computing have allowed for building of digital signal processors that are capable of performing computations to the order of a few hundred million operations per second (MOPS). These advances make it feasible to build cognitive systems that are capable of continuously monitoring the environment in which they operate and adapting to the environment. A cognitive radar should be capable of performing intelligent signal processing at *both* the transmitter *and* the receiver based on its knowledge of the environment. The radar may acquire this knowledge on the fly using the radar returns or use the prior knowledge of the environment.

Radars operating in urban environments suffer from the interference of multipath reflections. The received radar return will be a linear combination of delayed, attenuated, and Doppler shifted versions of the transmitted signal coming along various paths. The strength of the line-of-sight (LOS) component can be very weak and in some cases there may not be a LOS component due to the shadowing effect. A standard radar using only the LOS return for the tracking procedure may fail to provide an updated state estimate in such cases. Therefore, to obtain an improved estimate of the target state, the radar should be capable of exploiting the information in the non-LOS (NLOS) radar returns. It has been shown in [2] that exploiting the multipath propagation improves the radar detection and more recently the authors in [3] have discussed a tracking procedure that exploits the multipath environment by using the prior knowledge on the geometry of the environment.

In this paper, we propose a cognitive radar to exploit the spatial diversity offered by the multipath propagation. We use the knowledge acquired by the radar to separate the signals arriving through various paths. We construct a new measurement vector, which we refer to as a virtual measurement vector, by coherently combining the delayed versions of the separated signals. To estimate the delays, we discretize the delay Doppler plane into several grid points and solve a sparse reconstruction problem. We use the virtual measurement vector for target tracking based on sequential Bayesian inference. We employ Orthogonal Frequency Division Multiplexing (OFDM) signalling at the transmitter and predict the posterior Cramér Rao bound (PCRB) on the mean square error of the target state estimate as a function of the weights to be transmitted on each subcarrier bin. We then minimize the predicted value of the PCRB to obtain the optimal weights to be transmitted in the next pulse repetition interval (PRI).

The rest of the paper is organized as follows. In section II, we discuss the formulation of the problem and describe the tracking environment, signal and the state space models. In section III, we describe the construction of the virtual measurement vector, using the estimates of the target scattering coefficients and the delays corresponding to each path. This construction, along with the sequential Bayesian inference and the adaptive waveform design forms the cognitive part of the tracking procedure. In section IV, we describe the target tracking algorithm and the recursive computation of the PCRB. Numerical simulations are shown in section V and the conclusions follow in section VI.

Notation: Bold small letters denote vectors, bold capital letters denote matrices. $(\cdot)^T$, $(\cdot)^H$, $E[\cdot]$, $\hat{(\cdot)}$, $\boldsymbol{I}_M$, $\Re(\cdot)$, $\mathrm{Tr}(\cdot)$, $\|\cdot\|$, $\partial(\cdot)$, $\otimes$, and $\mathrm{vec}(\cdot)$ denote transpose, conjugate transpose, expectation operator, estimate, $M \times M$ identity matrix, real part, trace, Euclidean norm, partial differentiation operator, Kronecker product and vectorization operator, respectively.

II. Problem Formulation

A. Tracking Environment

We consider a point target moving in a rich urban environment. There are multiple reflecting surfaces in the region

This work was supported by the Department of Defense under the AFOSR MURI Grant FA9550-05-1-0443 and the ONR Grant N000140810849.

of interest, which may correspond to buildings or any other targets moving in the region. For wideband signalling, the received signal $y(t)$ can be expressed as a function of the transmitted signal $s(t)$ as

$$\begin{aligned} y(t) &= \sum_{p=0}^{P-1} y_p(t) \\ &= \sum_{p=0}^{P-1} \alpha_p s(\gamma_p(t-\tau_p)) + w(t) \end{aligned} \quad (1)$$

where α_p, τ_p, $\beta_p = \gamma_p - 1$ and $y_p(t)$ denote the complex target scattering coefficient, delay, Doppler and the received signal corresponding to the p^{th} path respectively, and $w(t)$ is the additive noise. The unknown parameters are related to the target range r and velocity $\boldsymbol{v}$ as $\tau_0 = \frac{2r}{c}$ and $\beta_p = \frac{2<\boldsymbol{v},\boldsymbol{u}_p>}{c}$, where c is the speed of the propagation and $\boldsymbol{u}_p$ is the direction of arrival unit vector along the p^{th} path. We assume that the radar is aware of the environment it is illuminating, and hence it knows the number of possible multipaths, P[1] in the region and the direction of arrival unit vectors, $\boldsymbol{u}_p$, along each path.

B. OFDM Measurement Model

We employ OFDM signalling [4] for the target tracking problem. The use of OFDM signals for radar problems was first proposed in [5]. Since then, several radar systems used OFDM signalling [6], [7]. OFDM divides the overall transmission bandwidth into smaller orthogonal frequencies (efficiently achievable using the fast fourier transform) and transmits the data over several narrow band channels having overlapping frequency spectra.

Let a_l be the transmitted symbol in the l^{th} subcarrier bin and B be the overall bandwidth of the transmission which is subdivided into L frequency bins corresponding to a subcarrier spacing of $\Delta f = B/L$. The transmitted signal $s(t)$, is then given as

$$s(t) = \sum_{l=0}^{L-1} a_l e^{2\pi l \Delta f t} u(t) \quad (3)$$

where

$$u(t) = \begin{cases} 1 & 0 \le t \le T_{\rm s} \\ 0 & \text{otherwise} \end{cases}$$

is a rectangular pulse function and $T_{\rm s}$ is the OFDM symbol duration. The equivalent pass band signal that is transmitted is given as

$$\tilde{s}(t) = 2\Re\{s(t)e^{2\pi f_{\rm c} t}\} \quad (4)$$

[1]If there are R reflecting surfaces in the environment and the radar returns with M bounces off these reflecting surfaces are considered significant, then an upper bound on the number of possible paths is given as

$$P = \left(\sum_{m=0}^{M} \sum_{i=0}^{m} P_i^R P_{M-i}^R \right) \quad (2)$$

where $P_i^R = \frac{R!}{(R-i)!}$ is the permutation of R objects taken i at a time. Of these, $m = 0$ corresponds to the LOS path and the others correspond to the NLOS paths. In practice, the signals arriving on paths with two or more bounces suffer severe attenuation.

where $f_{\rm c}$ is the carrier frequency. Using (4) in (1), the received signal can be written as

$$\begin{aligned} \tilde{y}(t) &= \sum_{p=0}^{P-1} \tilde{y}_p(t) \\ &= \sum_{p=0}^{P-1} 2\alpha_p \Re \left(\sum_{l=0}^{L-1} a_l e^{j2\pi f_l \gamma_p (t-\tau_p)} u(\gamma_p(t-\tau_p)) \right) \\ &+ \tilde{w}(t) \end{aligned} \quad (5)$$

where $f_l = f_{\rm c} + l\Delta f$. The equivalent baseband signal is given as

$$y(t) = \sum_{p=0}^{P-1} \alpha_p \sum_{l=0}^{L-1} a_l \phi_{p,p}(t,l) + w(t) \quad (6)$$

where
$\phi_{p_1,p_2}(t,l) = e^{-j2\pi f_l \gamma_{p_2} \tau_{p_1}} e^{j2\pi \beta_{p_2} f_l t} e^{j2\pi l \Delta f t} u(\gamma_{p_2}(t-\tau_{p_1}))$ and $w(t)$ is the circularly symmetric additive white Gaussian noise. The received signal is then sampled at the receiver at a rate $f_{\rm s} = \frac{1}{t_{\rm s}} = \frac{T_{\rm s}}{L}$ to obtain a discrete time signal given as

$$y[n] = \sum_{p=0}^{P-1} \alpha_p \sum_{l=0}^{L-1} a_l \phi_{p,p}(n,l) + w[n] \quad (7)$$

where $\phi_{p_1,p_2}(n,l) = e^{-j2\pi f_l \gamma_{p_2} \tau_{p_1}} e^{j2\pi \beta_{p_2} f_l n t_{\rm s}} e^{j2\pi n l/L} u_{p_1}[n]$. Assuming that $T_{\rm s}/\gamma_{p_2} \approx T_{\rm s}$, $u_{p_1}[n]$ is given as

$$u_{p_1}[n] = \begin{cases} 1 & \frac{\tau_{p_1}}{t_{\rm s}} \le n \le \frac{T_{\rm s}+\tau_{p_1}}{t_{\rm s}} \\ 0 & \text{otherwise} \end{cases}$$

Defining $\boldsymbol{\Phi}_p$ to be a $N \times L$ matrix whose elements are given by $\phi_{p,p}(n,l)$, (7) can be written in a matrix form as

$$\boldsymbol{y} = \boldsymbol{\Phi} \boldsymbol{A} \boldsymbol{\alpha} + \boldsymbol{w} \quad (8)$$

where
$\boldsymbol{y}$: $N \times 1$ is the received signal vector
$\boldsymbol{\Phi}$: $N \times LP$ matrix given by $\boldsymbol{\Phi} = [\boldsymbol{\Phi}_0, \boldsymbol{\Phi}_1, \cdots, \boldsymbol{\Phi}_{P-1}]$
$\boldsymbol{A}$: $LP \times P$ is a block diagonal matrix where each block is an $L \times 1$ column vector containing the transmitted weights on each sub carrier bin
$\boldsymbol{\alpha}$: $P \times 1$ column vector of the target scattering coefficients along each path and
$\boldsymbol{w}$: $N \times 1$ is the zero mean circularly symmetric complex additive white Gaussian noise which is assumed to be temporally uncorrelated with a known covariance matrix $\boldsymbol{\Sigma}_{\rm w} = \sigma_{\rm w}^2 \boldsymbol{I}_N$.

C. State Space Model

We consider a target moving with a constant velocity in a two dimensional plane and let x_k, y_k, $\dot{x}_k$ and $\dot{y}_k$ denote the position and velocity of the target in the x and the y direction respectively, in the k^{th} PRI. Thus the vector $\boldsymbol{\theta}_k = [x, y, \dot{x}, \dot{y}]^T$ completely characterizes the state of the target in the k^{th} PRI. The state equation for the target is given as

$$\boldsymbol{\theta}_{k+1} = \boldsymbol{H} \boldsymbol{\theta}_k + \boldsymbol{e}_k \quad (9)$$

where $\boldsymbol{e}$ denotes the error in the state modeling. When the target follows a linear trajectory, the state transition matrix $\boldsymbol{H}$ is given by

$$\boldsymbol{H} = \begin{bmatrix} \boldsymbol{I}_2 & T_{\rm p} \boldsymbol{I}_2 \\ \boldsymbol{0}_2 & \boldsymbol{I}_2 \end{bmatrix} \quad (10)$$

where T_p is the pulse repetition interval. The error in the measurement model is assumed to be Gaussian distributed with zero mean and a covariance matrix given by [8]

$$\boldsymbol{\Sigma}_e = \epsilon \begin{bmatrix} \frac{1}{3}T_\mathrm{p}^3\boldsymbol{I}_2 & \frac{1}{2}T_\mathrm{p}^2\boldsymbol{I}_2 \\ \frac{1}{2}T_\mathrm{p}^2\boldsymbol{I}_2 & T_\mathrm{p}\boldsymbol{I}_2 \end{bmatrix} \tag{11}$$

where ϵ is the intensity of the noise process.

The unknown target parameters are related to the state as $\tau_0 = \frac{2\sqrt{x^2+y^2}}{c}$ and $\beta_p = \frac{2<\boldsymbol{v},\boldsymbol{u}_p>}{c}$, where $\boldsymbol{v} = [\dot{x}, \dot{y}]^T$ and c is the speed of the propagation. Note that to use the measurement model (8) for tracking, we have to extract only the LOS component as the other unknown delays, $\tau_p, p = 1, 2, \ldots P-1$ cannot be explicitly related to target range. However, the inherent diversity is not exploited if only the LOS component is considered.

III. Virtual Measurement Vector

In this section, we describe the signal processing that is required at the receiver to construct a virtual measurement vector. The idea here is to linearly combine the delayed versions of the received signal along P different paths using the weight vector $\boldsymbol{\zeta} = [\zeta_0, \zeta_1, \ldots, \zeta_{P-1}]$. To this end, we construct a signal $\tilde{z}(t)$

$$\tilde{z}(t) = \sum_{p\prime=0}^{P-1} \zeta_{p\prime}\tilde{y}_{p\prime}(t+\tau'_{p\prime}) \tag{12}$$

and use it for obtaining the target state estimates. Ideally, the $p\prime^{th}$ term in the summation should be delayed by $\tau_{p\prime} - \tau_0$ to completely overlap with the LOS component. So, we choose

$$\tau'_{p\prime} = \tau_{p\prime} - \tau_0 \tag{13}$$

In order to coherently combine the signals, we choose the weights $\zeta_{p\prime} = \frac{1}{\alpha_{p\prime}}$. With these substitutions, and changing the summation index from $p\prime$ back to p for notational convenience, the equivalent base band version of the virtual measurement vector can be obtained as

$$z(t) = \sum_{p=0}^{P-1}\sum_{l=0}^{L-1} a_l\phi'_{p,p}(t,l) + v(t) \tag{14}$$

where $\phi'_p(t,l) = e^{-j2\pi f_l\gamma_p\tau_0}e^{j2\pi f_l\beta_p t}e^{j2\pi l\Delta f t}u\left(\gamma_p(t-\tau_0)\right)$. It can be seen that using the virtual measurement vector should provide a better performance since we are using the signals arriving on all the paths. Note that all the unknown parameters in the new measurement equation (14) can be related to the target state vector which was not the case using the measurement equation (6). The corresponding discrete time version of (14) is

$$\boldsymbol{z} = \boldsymbol{\Phi}'\boldsymbol{A}\boldsymbol{1} + \boldsymbol{v} \tag{15}$$

where $\boldsymbol{\Phi}' = [\boldsymbol{\Phi}'_0, \cdots, \boldsymbol{\Phi}'_{P-1}]$, where $\phi'_p(n,l) = e^{-j2\pi f_l\gamma_p\tau_0}e^{j2\pi f_l\beta_p nt_s}e^{j2\pi nl/L}u_0[n]$ and $\boldsymbol{1}$ represents a $P\times 1$ column vector of ones and $\boldsymbol{z}$ is the virtual measurement vector. Note that the new measurement model has a different noise covariance structure given as $\boldsymbol{\Sigma}_\mathrm{v} = \sigma_\mathrm{w}^2\sum_{p=0}^{P-1}\frac{1}{\alpha_p^2}\boldsymbol{I}_N$.

To construct the virtual measurement vector, we need the estimates of $\boldsymbol{\tau} = [\tau_0, \cdots, \tau_{P-1}]^T$ and $\boldsymbol{\alpha} = [\alpha_0, \cdots \alpha_{P-1}]^T$. Under the Gaussian white noise assumption, the maximum likelihood estimates of $\boldsymbol{\tau}$ and $\boldsymbol{\alpha}$ are given as

$$\hat{\boldsymbol{\tau}}, \hat{\boldsymbol{\alpha}} = \arg\min_{\boldsymbol{\tau},\boldsymbol{\alpha}} \sum_{n=0}^{N-1}\left\| y[n] - \sum_{p=0}^{P-1}\alpha_p\sum_{l=0}^{L-1}a_l\phi_p(n,l)\right\|^2 \tag{16}$$

Obtaining an estimate of $\boldsymbol{\tau}$ using the maximum likelihood approach becomes infeasible in this case because the delays corresponding to each path are closely spaced, which results in many local extrema [9]. Also, the estimate converges to a global minimum only if an excellent initial point is chosen. To find the estimates of the delay, the delay Doppler plane can be discretized into $M = M_1M_2$ grid points in the region of interest. Defining $\boldsymbol{s}_{m_1m_2} = \sum_{l=0}^{L-1} a_l\boldsymbol{\phi}_{m_1,m_2}(n,l)$ and $\boldsymbol{S} = [\boldsymbol{s}_{11}, \boldsymbol{s}_{12}, \cdots, \boldsymbol{s}_{M_1M_2}]$, where $\{\tau_{m_1}\}_{m_1=1}^{M_1}$ and, $\{\beta_{m_2}\}_{m_2=1}^{M_2}$ correspond to the grid points in the delay Doppler plane, (8) can be rewritten as

$$\boldsymbol{y} = \boldsymbol{S}\boldsymbol{\psi} + \boldsymbol{w} \tag{17}$$

where $\boldsymbol{S}$ is a $N\times M$ basis matrix and $\boldsymbol{\psi}$ is a $M\times 1$ sparse vector. If the true delays are among $\{\tau_m\}$, then the delay estimates are hidden in the non zero components of $\boldsymbol{\psi}$ [9]. This is a standard sparse reconstruction problem and there are several algorithms to solve this problem [10], [11]. We used the Dantzig selector [12] to solve the reconstruction problem. Specifically, we solved

$$\hat{\boldsymbol{\psi}} = \arg\min_{\boldsymbol{\psi}} \|\boldsymbol{\psi}\|_{l_1} \text{ s.t } \left\|\boldsymbol{S}^H(\boldsymbol{y}-\boldsymbol{S}\boldsymbol{\psi})\right\|_{l_\infty} \le \sigma_\mathrm{w}\sqrt{2\log(N)} \tag{18}$$

using the CVX package for solving the convex problems [13].

IV. Adaptive Target Tracking

Target tracking requires processing over multiple range cells to determine the exact target location in each iteration. In this section, we use the framework developed by the authors in [14] to implement an adaptive target tracking method based on the state space model (9) and the measurement model (15).

A. Particle filter for Target Tracking

A particle filter [15] is used for estimating the target state at each iteration. The posterior belief is approximated as a weighted sum of the samples drawn from a known proposal distribution.

$$p(\boldsymbol{\theta}_k \mid \boldsymbol{z}_{1:k}) \approx \sum_{i=1}^{\mathrm{N_s}} w_k^{(i)}\delta(\boldsymbol{\theta}_k - \boldsymbol{\theta}_k^{(i)}) \tag{19}$$

where $\boldsymbol{\theta}_k^{(i)}$ are the samples drawn from a known importance density function.

$$\boldsymbol{\theta}_k \sim q(\boldsymbol{\theta}_k|\boldsymbol{\theta}_{1:k-1}, \boldsymbol{z}_k) \tag{20}$$

The importance distribution $q(\boldsymbol{\theta}_k|\boldsymbol{\theta}_{1:k-1}, \boldsymbol{z}_k)$ is chosen to be the transitional prior $p(\boldsymbol{\theta}_k|\boldsymbol{\theta}_{1:k-1})$. This choice provides a simple recursive weight update equation.

$$\boldsymbol{w}_k \propto \boldsymbol{w}_{k-1}p(\boldsymbol{\theta}_k|\boldsymbol{z}_k) \tag{21}$$

B. Computation of the Posterior Cramér Rao Bound

Let $\Delta_{\boldsymbol{\eta}} = [\partial\eta_1, \partial\eta_2, \ldots \partial\eta_r]^T$ denote a vector of the partial derivatives with respect to the vector $\boldsymbol{\eta}$ and $\Delta_{\upsilon}^{\kappa} = \Delta_{\upsilon}\Delta_{\kappa}^T$ denote the partial derivative vectors. With this notation the PCRB for an unbiased estimate of $\boldsymbol{\theta}$ has the form [16]

$$E[(\boldsymbol{\theta} - \hat{\boldsymbol{\theta}})(\boldsymbol{\theta} - \hat{\boldsymbol{\theta}})^T] \geq \boldsymbol{J}^{-1} \tag{22}$$

where $\boldsymbol{J}$ is the Fisher information matrix (FIM) given as

$$\boldsymbol{J} = -E[\Delta_{\theta}^{\theta} \log(p(\boldsymbol{\theta}, \boldsymbol{z}))] \tag{23}$$

C. Adaptive Design and Recursive Update of the Fisher Information Matrix

We use the recursive equation in [16] for the computation of the FIM in the pulse interval k. It was shown that

$$\boldsymbol{J}_{k+1}(\boldsymbol{a}_{k+1}) = \left[\boldsymbol{\Sigma}_{\mathrm{v}} + \boldsymbol{H}\boldsymbol{J}_k(\boldsymbol{a}_k)^{-1}\boldsymbol{H}^T\right]^{-1} + \boldsymbol{\Gamma}_{k+1}(\boldsymbol{a}_{k+1}) \tag{24}$$

where

$$\boldsymbol{\Gamma}_{k+1} = E[\Delta_{\boldsymbol{\theta}_{k+1}}^{\boldsymbol{\theta}_{k+1}} \log(p(\boldsymbol{\theta}_{k+1}, \boldsymbol{z}_{k+1}))] \tag{25}$$

$\boldsymbol{a}_k$, $\boldsymbol{a}_{k+1}$ are the waveform parameters in the pulse interval k and $k+1$, $\boldsymbol{\Sigma}_{\mathrm{v}}$ is the covariance of the process noise and $\boldsymbol{H}$ is the transition matrix of the state parameters. The expectation in (25) does not have a closed form solution and it can be evaluated numerically by drawing samples from the distribution $p(\boldsymbol{\theta}_{k+1}|\boldsymbol{z}_{k+1})$ [14]. From (15), $p(\boldsymbol{\theta}_{k+1}|\boldsymbol{z}_{k+1}) = \mathbb{C}\mathcal{N}(\boldsymbol{\Phi}'\boldsymbol{A}\mathbf{1}, \boldsymbol{\Sigma}_{\mathrm{v}})$. The approximation for $\boldsymbol{\Gamma}_{k+1}$ is then given as

$$\boldsymbol{\Gamma}_{k+1} \approx \sum_{i=1}^{\mathrm{N_s}} w_k^{(i)} \boldsymbol{\Xi}_{k+1}\left(\boldsymbol{a}_{k+1}^{(i)}\right). \tag{26}$$

where $\boldsymbol{\Xi}_{k+1} = E_{\boldsymbol{z}_{k+1}|\boldsymbol{\theta}_{k+1}}\left[-\triangle_{\boldsymbol{\theta}_{k+1}}^{\boldsymbol{\theta}_{k+1}} \log p(\boldsymbol{z}_{k+1} \mid \boldsymbol{\theta}_{k+1})\right]$ and $\boldsymbol{\theta}_{k+1}^{(i)}$ are the samples drawn from $p(\boldsymbol{\theta}_{k+1} \mid \boldsymbol{\theta}_k^{(i)})$. The optimal waveform transmitted in the next symbol interval is then obtained by solving the optimization problem.

$$\boldsymbol{a}_{k+1}^{*} = \arg \min_{\boldsymbol{a}_{k+1} \in \mathcal{R}^L} \mathrm{Tr}\{J_{k+1}^{-1}(\boldsymbol{a}_{k+1})\} \text{ subject to } \boldsymbol{a}^H\boldsymbol{a} = 1 \tag{27}$$

For the measurement model described in (15), the expectation $E_{\boldsymbol{z}_{k+1}|\boldsymbol{\theta}_{k+1}}\left[-\triangle_{\boldsymbol{\theta}_{k+1}}^{\boldsymbol{\theta}_{k+1}} \log p(\boldsymbol{z}_{k+1} \mid \boldsymbol{\theta}_{k+1})\right] = [\xi_{ij}]$, where

$$\begin{aligned}\xi_{ij} \quad = \quad & \left(\frac{\partial}{\partial\theta_i}\mathrm{vec}(\boldsymbol{\Phi}')\right)^H \left(\mathbf{1}^T\boldsymbol{A}^T \otimes \boldsymbol{I}_N\right)^H \boldsymbol{\Sigma}_{\mathrm{v}}^{-1} \\ & \left(\mathbf{1}^T\boldsymbol{A}^T \otimes \boldsymbol{I}_N\right) \frac{\partial}{\partial\theta_j}\mathrm{vec}(\boldsymbol{\Phi}')\end{aligned} \tag{28}$$

V. Numerical Results

We present numerical results to demonstrate the improvement obtained using a cognitive tracking approach over the standard radar. We consider a 2D scenario, where the target is moving in a linear trajectory starting at the location $(10\text{km}, 10\text{km})$. The radar had a constant velocity $(100\text{m/s}, 100\text{m/s})$. The state covariance matrix was chosen according to (11) and we have chosen an ϵ value of 8×10^2. We used the following parameters for the simulations.

- Carrier frequency (f_{c}) = 1Ghz
- Bandwidth (B) = 100Mhz
- Number of subcarriers (L) = 16 corresponding to a subcarrier spacing (Δf) of 6.25Mhz

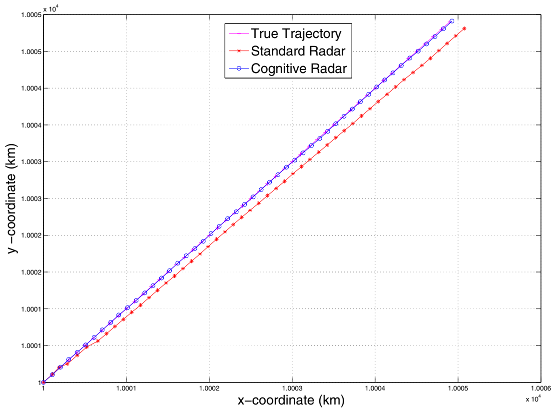

Fig. 1. Comparison of tracking results for standard and cognitive radar

- Number of multipaths (P) = 3
- Pulse repetition interval (T_{p}) = 1ms

For a standard radar, we used a window of 250 samples from the measurement vector around the predicted range. All the sub carriers were loaded with equal weights subject to the constraint $\boldsymbol{a}^H\boldsymbol{a} = 1$. The noise variance σ_{w}^2 was chosen to achieve the required Signal to Noise Ratio (SNR) defined as

$$\mathrm{SNR} = \frac{(\boldsymbol{\Phi}\boldsymbol{A}\boldsymbol{\alpha})^{\mathrm{H}}(\boldsymbol{\Phi}\boldsymbol{A}\boldsymbol{\alpha})}{\sigma_{\mathrm{w}}^2} \tag{29}$$

For a cognitive radar, we used a window of 250 samples from the virtual measurement vector around the predicted range. The weights to be transmitted on each sub carrier in each PRI were obtained by solving (27). The noise variance σ_{v}^2 was chosen to be $\sum_{p=0}^{P-1}(\frac{1}{\alpha_p})^2\sigma_{\mathrm{w}}^2$. All the simulations were run at an SNR of 25dB. The target scattering coefficients in each pulse repetition interval were chosen to be $[0.4\varsigma_1, 0.7\varsigma_2, 0.5\varsigma_3]$ where ς_1, ς_2 and ς_3 were drawn from a $\mathbb{C}\mathcal{N}(0, 1)$. The delays ($\tau_p$) are chosen such that the received signal is a linear combination of three non-overlapping pulses arriving along the three multipaths. The Doppler (β_p) were chosen by randomly generating three unit vectors corresponding to the direction of arrival in each path.

The estimated target trajectories using a standard radar and a cognitive radar are shown in Fig. 1. The mean square error for the range and the velocity estimates in PRI are shown in Fig. 2 and Fig. 3. From the figures, it can be seen that when the LOS component had less strength relative to the NLOS components, the standard radar failed to use the measurement information to obtain an updated value of the target state estimate. The measurement vector does not provide any new information and the best the radar can do is to use the predicted value. Cognitive radar, on the other hand, exploits the multipath and waveform diversity and hence performs better.

VI. Conclusions

We considered the problem of target tracking in a multipath scenario and used a particle filter for the tracking algorithm. In each Pulse repetition Interval (PRI), the radar estimated the delay, Doppler and the target scattering coefficients and used this information to construct a virtual measurement vector. In

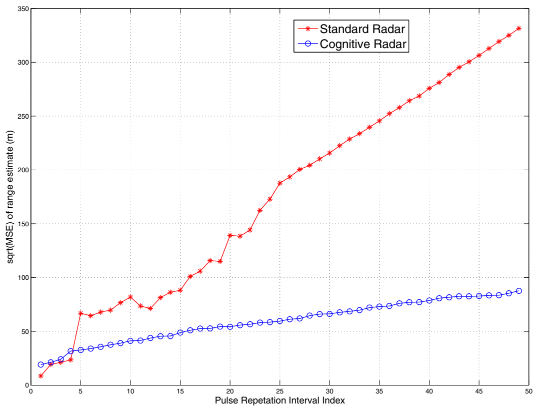

Fig. 2. Square root of MSE for range estimates

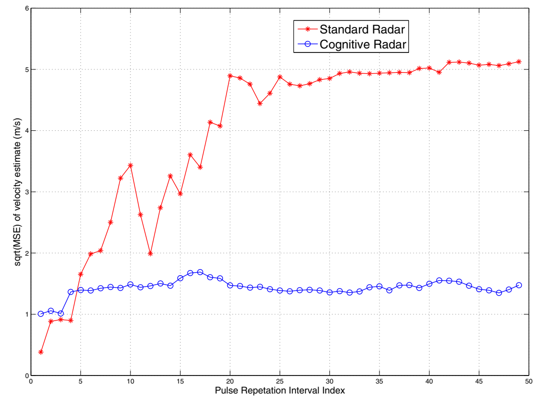

Fig. 3. Square root of MSE for velocity estimates

addition to exploiting the diversity offered by the multipath environment, the use of the virtual vector eliminated the problem of deriving an explicit relation between the delay corresponding to each multipath and the target range. We used adaptive waveform design by minimizing the posterior Cramér Rao bound on the target state estimate to find the optimal weights to be transmitted on each subcarrier bin of the Orthogonal Frequency Division Multiplexing signal in the next PRI. We demonstrated through numerical simulations that the use of cognitive radar offers significant improvement over the standard radar.

REFERENCES

[1] S. Haykin, "Cognitive radar: A way of the future," *Signal Processing Magazine, IEEE*, vol. 23, no. 1, pp. 30–40, 2006.

[2] J. L. Krolik, J. Farrell, and A. Steinhardt, "Exploiting multipath propagation for GMTI in urban environments," in *IEEE Conference on Radar*. Verona, Newyork: IEEE, Apr. 24-27, 2006, pp. 65–68.

[3] B. Chakraborty, Y. Li, J. J. Zhang, T. Trueblood, A. Papandreou-Suppappola, and D. Morrell, "Multipath exploitation with adaptive waveform design for target tracking in urban terrain," in *International Conference on Acoustics, Speech, and Signal Processing*. Dallas, Texas: IEEE, Mar. 14-19, 2010, pp. 3894–3897.

[4] A. Pandharipande, "Principles of OFDM," *IEEE Potentials*, vol. 21, no. 2, pp. 16–19, Apr. 2002.

[5] M. Jankiraman, B. J. Wessels, and P. van Genderen, "System design and verification of the PANDORA multifrequency radar," in *Proceedings of International Conference on Radar Systems*. Brest, France: IEEE, May 17-21, 1999.

[6] S. Sen, M. Hurtado, and A. Nehorai, "Adaptive OFDM radar for detecting a moving target in urban scenarios," in *International Waveform Diversity and Design Conference*. Orlando, Florida: IEEE, Feb. 2009, pp. 268–272.

[7] S. Sen and A. Nehorai, "Target detection in clutter by an adaptive OFDM radar," *IEEE Signal Processing Letters*, vol. 16, pp. 592–595, Jul. 2009.

[8] Y. Bar-Shalom, X.-R. Li, and T. Kirubarajan, *Estimation with Applications to Tracking and Navigation*. New York: Wiley, 2001.

[9] J.-J. Fuchs, "Multipath time-delay detection and estimation," *IEEE Trans. on Signal Processing*, vol. 47, no. 1, pp. 237–243, Jan 1999.

[10] D. L. Donoho, M. Elad, and V. N. Temlyakov, "Stable recovery of sparse overcomplete representations in the presence of noise," *IEEE Trans. on Information Theory*, vol. 52, no. 1, pp. 6–18, Jan. 2006.

[11] P. Boufounos, M. F. Duarte, and R. G. Baraniuk, "Sparse signal reconstruction from noisy compressive measurements using cross validation," in *IEEE/SP 14th Workshop on Statistical Signal Processing*, Aug. 2007, pp. 299–303.

[12] E. J. Candés and T. Tao, "The Dantzig selector: Statistical estimation when p is much larger than n," *Annals of Statistics*, vol. 35, no. 6, pp. 2313–2351, 2007.

[13] M. Grant and S. Boyd, "CVX: Matlab software for disciplined convex programming," Stanford University, http://stanford.edu/boyd/cvx, web page and software, Jun. 2009.

[14] M. Hurtado, T. Zhao, and A. Nehorai, "Adaptive polarized waveform design for target tracking based on sequential Bayesian inference," *IEEE Trans. on Signal Processing*, vol. 56, pp. 1120–1133, Mar. 2008.

[15] M. S.Arulampalam, S. Maskell, N. J. Gordon, and T. Clapp, "A tutorial on particle filters for online nonlinear/non-Gaussian Bayesian tracking," *IEEE Trans. on Signal Processing*, vol. 50, no. 2, pp. 174–188, Feb. 2002.

[16] P. Tichavsk, C. H. Muravchik, and A. Nehorai, "Posterior Cramér-Rao bounds for discrete-time nonlinear filtering," *IEEE Trans. on Signal Processing*, vol. 46, no. 5, May 1998.